Fragmentation of valence electronic states of CHF 2CF 3 + studied by threshold photoelectron–photoion coincidence (TPEPICO) techniques in the photon energy range 12–25 eV

ARTICLE *in* CHEMICAL PHYSICS · OCTOBER 2002

Impact Factor: 1.65 · DOI: 10.1016/S0301-0104(02)00790-5

4 AUTHORS, INCLUDING:

Weidong Zhou
Zhejiang Normal University
37 PUBLICATIONS **292** CITATIONS

SEE PROFILE

Richard P Tuckett
University of Birmingham
162 PUBLICATIONS **2,059** CITATIONS

SEE PROFILE

ELSEVIER

Chemical Physics 283 (2002) 419–431

Chemical Physics

www.elsevier.com/locate/chemphys

Fragmentation of valence electronic states of $CHF_2CF_3^+$ studied by threshold photoelectron–photoion coincidence (TPEPICO) techniques in the photon energy range 12–25 eV

Weidong Zhou [a], D.P. Seccombe [a,1], R.P. Tuckett [a,*], M.K. Thomas [b]

[a] *School of Chemical Sciences, University of Birmingham, Edgbaston, Birmingham, B15 2TT, UK*
[b] *Department of Physics, University of Reading, Whiteknights, Reading, RG6 2AG, UK*

Received 20 February 2002

Abstract

Vacuum ultraviolet synchrotron radiation and threshold photoelectron–photoion coincidence (TPEPICO) spectroscopy have been used to study the decay dynamics of the valence electronic states of $CHF_2CF_3^+$. The threshold photoelectron spectrum (TPES) and ion yield curves of the observed fragments have been recorded in the photon energy range 12–25 eV. Electrons and ions are detected by threshold electron analysis and time-of-flight (TOF) mass spectrometry, respectively. Using a combination of the measured TPES and ab initio molecular orbital calculations, we conclude that the $CHF_2CF_3^+$ cation adopts a staggered C_s geometry, the $\tilde{X}\ ^2A'$ ground state being formed by electron removal from the 18a′ σ-bonding orbital of CHF_2CF_3. Upon ionisation, large geometry changes and broad spectral bands are both predicted and observed. The next outer-valence orbitals of CHF_2CF_3, 17a′ and 11a″, are predominantly associated with fluorine 2p orbitals located on the CHF_2 group. Translational kinetic energy releases are determined from fixed-energy TPEPICO-TOF spectra. The ground state of $CHF_2CF_3^+$ dissociates through C–C bond cleavage with a relatively small release of energy. By contrast the $\tilde{A}$ and $\tilde{B}$ states dissociate rapidly by an impulsive mechanism with a larger fractional release of energy to $CHFCF_3^+ + F$. Upper limits for the ionisation threshold of CHF_2CF_3 (12.70 ± 0.05 eV) and the enthalpy of formation of $CHFCF_3^+$ at 298 K (299 ± 7 kJ mol^{-1}) are determined.

1. Introduction

In order to avoid further ozone depletion in the stratosphere, chlorofluorocarbons (CFCs) are increasingly being replaced by hydrofluorocarbons (HFCs) and hydrochlorofluorocarbons (HCFCs), because of their less adverse effects on the stratospheric ozone layer [1]. At present both industrial

* Corresponding author. Tel.: +44-121-414-4425; fax: +44-121-414-4426.
E-mail address: r.p.tuckett@bham.ac.uk (R.P. Tuckett).
[1] Present address : Physics Department, Newcastle University, Newcastle-upon-Tyne, NE1 7RU, UK.

0301-0104/02/$ - see front matter
PII: S0301-0104(02)00790-5

and scientific attention is strongly focused on the HFCs, because the presence of chlorine atoms in HCFCs can still have a deleterious effect on ozone [2]. The growing importance of HFCs has prompted a number of recent studies to determine their physical and chemical properties, as well as to understand their chemical behaviour in the atmosphere [3–8]. Even though HFCs do not destroy the ozone layer, they still pose a threat to the environment because of their potential to contribute to global warming. The lifetimes of these species in the atmosphere can be very long due to their slow reaction with important tropospheric free radicals such as $OH^{\cdot}$ and $O(^1D)$, and the removal of these species from the atmosphere may be governed by photoionisation and photodissociation processes that occur in the mesosphere. The vacuum-UV (VUV) photochemistry of these molecules has therefore aroused much interest, and an understanding of the decay dynamics of Rydberg states of the neutral molecule and excited valence states of the parent molecular ion can provide useful information.

An ongoing aim of our group is to investigate the decay dynamics of the valence states of a number of HFC and other halocarbon cations, using synchrotron radiation as a tunable VUV photoionisation source. We have recently reported studies of a series of saturated and unsaturated perfluorocarbons (PFCs) using threshold photoelectron–photoion coincidence (TPEPICO) techniques [9,10]. The decay dynamics of the parent cations, $C_xF_y^+$, was probed, and some thermodynamic data were derived. Although several publications have dealt with the experimental and theoretical determination of the structure, the rotational barrier, and the atmospheric reactions of pentafluoroethane (CHF_2CF_3) [11–18], there have been almost no attempts to probe the unimolecular dissociation dynamics of the molecule or its parent cation. This includes the absence of a photoelectron spectrum (PES), photoionisation mass spectrum (PIMS), or electron impact (EI) studies. In this paper, the first of a series of investigations of HFC cations using synchrotron radiation, we describe the results of a TPEPICO study of CHF_2CF_3 from the onset of ionisation (ca. 12.6 eV) up to 25 eV. The first observations of the threshold photoelectron spectrum (TPES) of CHF_2CF_3 and the state-selected fragmentation of the parent ion are presented. From these measurements a breakdown diagram is obtained, yielding the formation probability of fragment ions as a function of photon energy. The mean translational kinetic energy releases in unimolecular fragmentations proceeding via a single bond cleavage are determined, and compared with the predictions of statistical and dynamical impulsive models. Some thermochemical data for the daughter ions of $CHF_2CF_3^+$ are also determined.

2. Theoretical and experimental methods

2.1. Computational methods

Ab initio molecular orbital calculations have been carried out using the quantum chemistry program GAUSSIAN 98 for CHF_2CF_3, both in its neutral ground state and in its cationic ground state generated by one-electron ionisation. The molecular structures for both species were optimised using the second-order Møller–Plesset theory (MP2) with the 6-31G(d) basis set, and all electrons were included at the MP2(full)/6-31G(d) level. The MP2(full)/6-31G(d) structures were then employed for energy calculations according to the Gaussian-2 (G2) theoretical procedure [19]. This procedure involves single-point total energy calculations at the MP4/6-311G(d,p), QCISD(T)/6-311g(d,p), MP4/6-311G(d,p), MP4/6-311G(2df,p), and MP2/6-311G(3df,2p) levels. A small empirical correction is employed to include the high-level correlation effects in the calculations of the total electronic energies (EE). The HF/6-31G(d) harmonic vibrational frequencies, scaled by 0.8929, are applied for zero-point vibrational energy (ZPVE) corrections to obtain the total energies at 0 K (E_0 = EE + ZPVE). The enthalpies of formation at 298 K ($\Delta_f H^0_{298}$) for molecular species are calculated using the scaled HF/6-31G(d) harmonic frequencies. The agreement between the G2 and experimental results is usually well within ± 0.15 eV (or ± 15 kJ mol^{-1}) [19].

2.2. Experimental methods

The coincidence apparatus for our TPEPICO experiments has been described in detail elsewhere [20,21], and is only outlined here. Synchrotron radiation from the 2 GeV electron storage ring at the Daresbury Laboratory is energy-selected using a 1 m Seya-Namioka monochromator equipped with two gratings, covering the energy range ca. 8–40 eV. All the experiments presented here were performed with the higher-energy grating (range 105–30 nm (12–40 eV), blaze ca. 55 nm). The optical resolution employed for the experiment is 0.3 nm. The wavelength of the monochromator was calibrated with the energies of the $^2P_{3/2}$ (15.759 eV) and $^2P_{1/2}$ (15.937 eV) states of Ar^+. The monochromatised VUV radiation is admitted into an interaction region through a glass capillary, and the photon flux is monitored using a photomultiplier tube via the visible fluorescence from a sodium salicylate-coated window behind the interaction region. In our experiments, the effects of second-order radiation are insignificant, since the energy of the ground electronic state of $CHF_2CF_3^+$ lies above that where second-order effects on this beamline are important.

Threshold photoelectrons and fragment cations produced by photoionisation were extracted in opposite directions by a 20 V cm^{-1} electric field applied across the interaction region, and detected separately by a channeltron electron multiplier and microchannel plates. The threshold electron analyser consists of a cylindrical electrostatic lens designed with large chromatic aberrations and a 127° post-analyser to reject energetic electrons emitted on axis. The operating resolution is now 10 meV [21], degraded from the initial design of ca. 3 meV [20] by increasing the size of the aperture to the post-analyser to enhance collection efficiency and hence sensitivity. Positive ions extracted from the interaction region are accelerated through a linear time-of-flight (TOF) mass spectrometer, which consists of a two-stage acceleration region configured to satisfy the space focusing condition [22] followed by a field-free region of length 186 mm. Pulses from the electron and ion detectors pass through discriminator and pulse shaping circuits to a time-to-digital converter (TDC) configured in the multi-hit mode. The electrons provide the start, the ions the stop pulses, allowing signals from the same ionisation process to be detected in delayed coincidence.

TPEPICO spectra can be recorded either continuously as a function of photon energy or at a fixed-energy. In the scanning-energy mode, flux-normalised TPEPICO spectra are recorded as three-dimensional histograms, where the coincidence count is plotted against both ion flight time and photon energy. By taking cuts through the histogram in different ways, two kinds of spectra are obtained. A cut through the map at a fixed photon energy yields the time-of-flight mass spectrum (TOF-MS), which identifies the fragment ions formed in the dissociative photoionisation at that energy. Alternatively, a background-subtracted cut taken through the histogram at a fixed ion flight time corresponding to a mass peak in the TOF-MS gives an ion yield curve. The breakdown diagram, yielding the formation probability of the product ions as a function of the photon energy, can then be calculated through normalisation of the ion intensities at every wavelength. In this mode of operation, the TOF resolution is degraded so that *all* the fragment ions are observed simultaneously. The threshold electron and total ion count produced during photoionisation are also recorded, yielding the TPES and total ion yield curve, respectively. By contrast, fixed-energy TOF spectra, measured at energies corresponding to peaks in the TPES, use a TOF resolution as high as the signal level permits, and often only one fragment ion is observed per spectrum. Fragment ions often have enough translational energy released for the peaks to be substantially broadened. It is then possible to obtain kinetic energy release distributions (KERDs) and hence mean kinetic energy releases $\langle KE \rangle_T$ from an analysis of the TOF-MS peak shape [23,24].

The sample gas CHF_2CF_3 was obtained commercially (Fluorochem, UK), with a stated purity of >99% and used without further purification. The sample was injected through a needle valve, and the operating pressure was ca. 5×10^{-5} Torr, several orders of magnitude above the chamber base pressure of 5×10^{-8} Torr.

3. Theoretical results

The optimised geometry of CHF_2CF_3 has been determined at the MP2/6-31G(d) level. The minimum energy geometrical parameters indicate that the molecule adopts a staggered structure of C_s symmetry with four atoms (C1, C2, H, F) lying in the symmetry plane. Values of the structural parameters and the G2 energies are listed in Table 1. The calculated values for the structural parameters are very close to the results of electron diffraction [25] and microwave [16] studies, and also agree with those determined by a recent ab initio calculation [13]. This agreement gives us confidence to apply the optimisation procedure to the cation. Like the neutral molecule, in a fully unconstrained calculation the parent cation is also predicted to have a staggered structure of C_s symmetry with four atoms located in the symmetry plane. The calculated geometrical parameters and G2 energy of the ground electronic state of $CHF_2CF_3^+$ ($\tilde{X}\ ^2A'$) are also listed in Table 1. 18 real vibrational frequencies are calculated for the cation, 11 with a′ symmetry (166, 213, 477, 592, 668, 820, 999, 1232, 1371, 1629 and 3384 cm^{-1}) and 7 with a″ symmetry (42, 148, 291, 588, 1394, 1612 and 1667 cm^{-1}). The absence of imaginary frequencies confirms that this C_s structure is stable.

Table 1
Calculated minimum energy geometry for neutral and cationic ground state of CHF_2CF_3

	Molecule CHF_2CF_3 $\tilde{X}\ ^1A'$	Cation $CHF_2CF_3^+$ $\tilde{X}\ ^2A'$
Symmetry:	C_s	C_s
R(C1,C2)	1.5187	1.9756
R(C1,F1)	1.3442	1.2906
R(C1,F2)	1.3442	1.2906
R(C1,F3)	1.3378	1.2884
R(C2,F4)	1.3575	1.2892
R(C2,F5)	1.3575	1.2892
R(C2,H)	1.0915	1.0955
∠C2C1F1	109.6342	101.8649
∠C2C1F2	109.6342	101.8649
∠C2C1F3	111.0334	101.6696
∠F1C1F2	108.6047	115.09216
∠F1C1F3	108.9453	115.9343
∠F2C1F3	108.9453	115.9343
∠C1C2F4	108.1626	101.55
∠C1C2F5	108.1626	101.55
∠C1C2H	111.5291	98.2977
∠F4C2F5	109.2811	115.1461
∠F4C2H	109.8263	117.6027
∠F5C2H	109.8263	117.6027
D(F1C1C2F4)	61.3044	60.4932
D(F1C1C2F5)	179.5573	179.4688
D(F1C1C2H)	−59.5691	−60.019
D(F2C1C2F4)	−179.5573	−179.4688
D(F2C1C2F5)	−61.1265	−60.4932
D(F2C1C2H)	59.5691	60.019
D(F3C1C2F4)	−59.1265	−59.4878
D(F3C1C2F5)	59.1265	59.4878
D(F3C1C2H)	180.0	180.0
G2 (E_0) (hartree)	−575.436763	−574.986438
AIE (eV)	12.25	

Bond angles in Å, bond angles in degrees.

The outer-shell electronic configuration of CHF_2CF_3 ($\tilde{X}\ ^1A'$) is $\ldots\ldots(9a'')^2(10a'')^2(11a'')^2(17a')^2(18a')^2$. The structure of the neutral molecule and its three highest outer-valence molecular orbitals (MOs) are shown in Fig. 1. It is difficult to give a simple characterisation of these MOs due to their hybridised nature. The highest-occupied molecular orbital (HOMO) of symmetry 18a′ is formed from s orbitals on carbon atoms and p orbitals on both fluorine and carbon atoms. It shows strong C–C σ bonding character, with some components of C–H and C–F σ bonding. Removal of an electron from this orbital yields the $\tilde{X}\ ^2A'$ ground state of $CHF_2CF_3^+$. The orbital of next highest energy (i.e., HOMO-1), 17a′, is largely localised on the CHF_2 group. This orbital has considerable fluorine 2p lone pair character, with some π and C–H σ-bonding contributions. The (HOMO-2) orbital, 11a″, is also localised on the CHF_2 group. It is of predominantly fluorine 2p lone pair character, with a weak antibonding interaction between the F atoms.

The computed geometries indicate that, whilst there is only little change in the C–H bond length upon ionisation to the ground state of the parent cation, considerable changes in the C–C (+0.46 Å), and to a lesser extent C–F (−0.06 Å), bond lengths are predicted. There is also a significant change in all bond angles at this level of theory. The increase of 0.46 Å in the C–C bond length is consistent with the 18a′ molecular orbital showing strong C–C σ-bonding character. Thus, loss of an electron

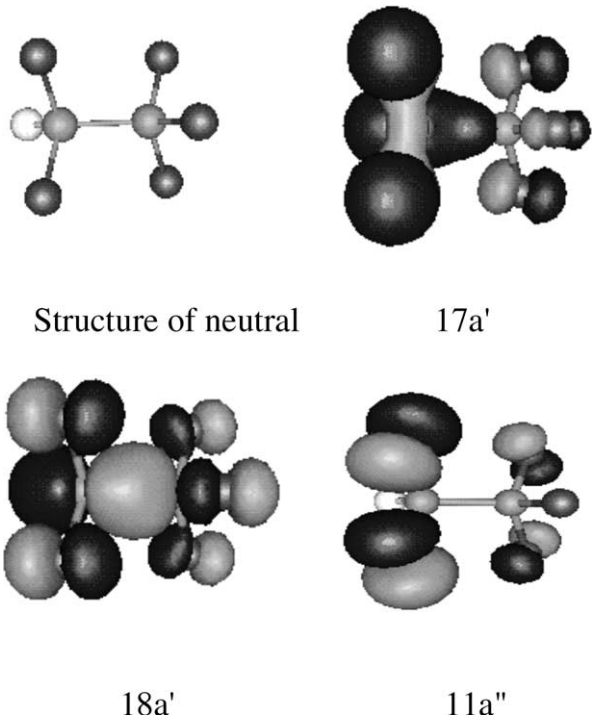

Fig. 1. Computed minimum energy structure of CHF_2CF_3 $\tilde{X}\ ^1A'$, and its three highest valence molecular orbitals. The orbitals are calculated at the MP2/6-31(d) level of theory.

from this orbital to form $CHF_2CF_3^+$ $\tilde{X}\ ^2A'$ leads to a major change in geometry. In addition to this enormous increase in the C–C bond length, both the CF_3 and CHF_2 groups become planar with the positive charge localised on them. Indeed, the computed structure of $CHF_2CF_3^+$ $\tilde{X}\ ^2A'$ is consistent with a resonance between the weakly bound complexes $CHF_2\cdots CF_3^+$ and $CHF_2^+\cdots CF_3$. Clearly, from the Franck–Condon principle, major vibrational excitation of the cation would be expected upon ionisation, particularly in the C–C stretching mode but also in the CHF_2 and CF_3 umbrella modes. The former mode is likely to lead to fragmentation of $CHF_2CF_3^+$ $\tilde{X}\ ^2A'$ to $CHF_2 + CF_3^+$ and $CHF_2^+ + CF_3$. The unfavourable Frank–Condon factors in the region of onset of the first photoelectron band of CHF_2CF_3 will almost certainly lead to a significant overestimation of the adiabatic ionisation energy (AIE) from the TPES [26]. From the G2 values for E_0 of CHF_2CF_3 and its parent cation, the AIE of CHF_2CF_3 is calculated to be 12.25 eV. This value is ca. 0.5 eV lower than the observed onset of signal in the TPES (Section 4). Similarly, a vertical ionisation energy (VIE) of 13.79 eV can be determined from the G2 energy difference between CHF_2CF_3 and $CHF_2CF_3^+$, calculated at the geometry of the neutral molecule. This value is in excellent agreement with the observed VIE 13.76 ± 0.05 eV (Section 4).

Because the 11a″ and 17a′ orbitals are extensively located on fluorine atoms, C–F bond fission would be expected to result from the removal of an electron from one or both of these orbitals, provided dissociation follows a rapid impulsive mechanism.

4. Experimental results and discussion

4.1. Threshold photoelectron spectrum

The TPES of pentafluoroethane has been measured at an optical resolution of 0.3 nm over the

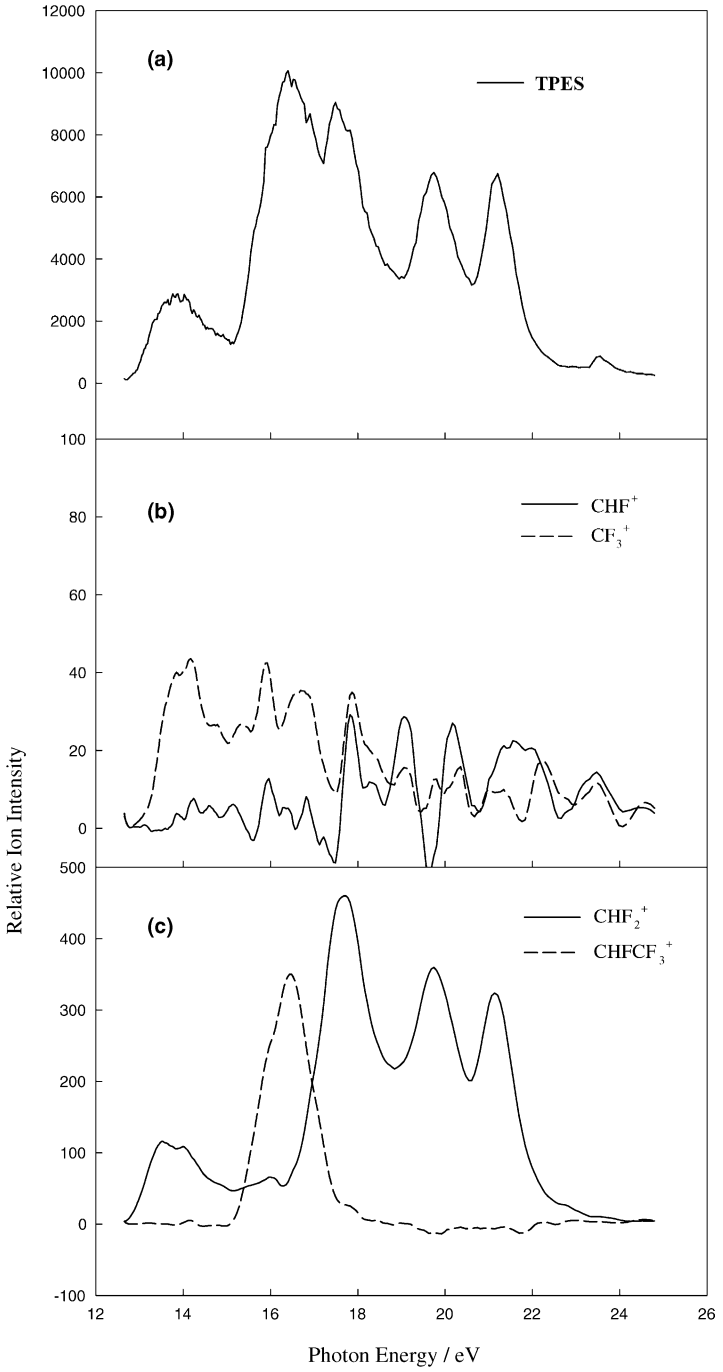

Fig. 2. (a) TPES of CHF_2CF_3; (b) and (c) coincidence ion yield curves. The optical resolution is 0.3 nm in all spectra.

energy range 12.5–24.8 eV (Fig. 2(a)). The resolution of the spectrum is determined by that of the photon source, not that of the electron analyser. The band at lowest energy, corresponding to formation of $CHF_2CF_3^+$ $\tilde{X}\ ^2A'$, has a maximum intensity at 13.76 ± 0.05 eV. From the molecular orbital calculation, it is clear that this state is produced through the loss of a C–C σ-bonding electron. This phenomenon is also observed with other fluorinated ethanes [7,9,27], and is consistent with the argument that fluorine substitution stabilises the C–H bonds more effectively than the C–C bond [27].

The TPES of pentafluoroethane has a similar relative intensity of ground and excited ionic states to that of C_2F_6 [9,28]. The observed onset of ionisation to $CHF_2CF_3^+$ $\tilde{X}\ ^2A'$ is 12.70 ± 0.05 eV. This value is ca. 0.5 eV higher than the calculated AIE of CHF_2CF_3. As noted above, this discrepancy shows the limitation of using the TPES to determine the ionisation threshold of a molecule that has a small Franck–Condon factor at threshold [26], and this experimental value only yields an upper limit to the AIE of CHF_2CF_3 at 298 K. We should also note that the onset of ionisation to $CHF_2CF_3^+$ is ca. 0.5 eV lower than that into the ground state of $C_2F_6^+$ [9,28].

The first and second excited states of $CHF_2CF_3^+$ correspond to the loss of an electron from the 2pπ non-bonding orbitals on the fluorine atoms of the $-CHF_2$ group. This is similar to the case for the $\tilde{A}$ and $\tilde{B}$ states of $C_2F_6^+$ [9,28,29]. It is therefore not surprising that these two molecules show similar photoelectron spectra in the range 15–19 eV. Indeed, the TPES of CHF_2CF_3 and C_2F_6 are remarkably similar in the higher energy range of 19–24 eV. Presumably this shows that the nature of lower-lying valence orbitals of C_2F_6 is relatively

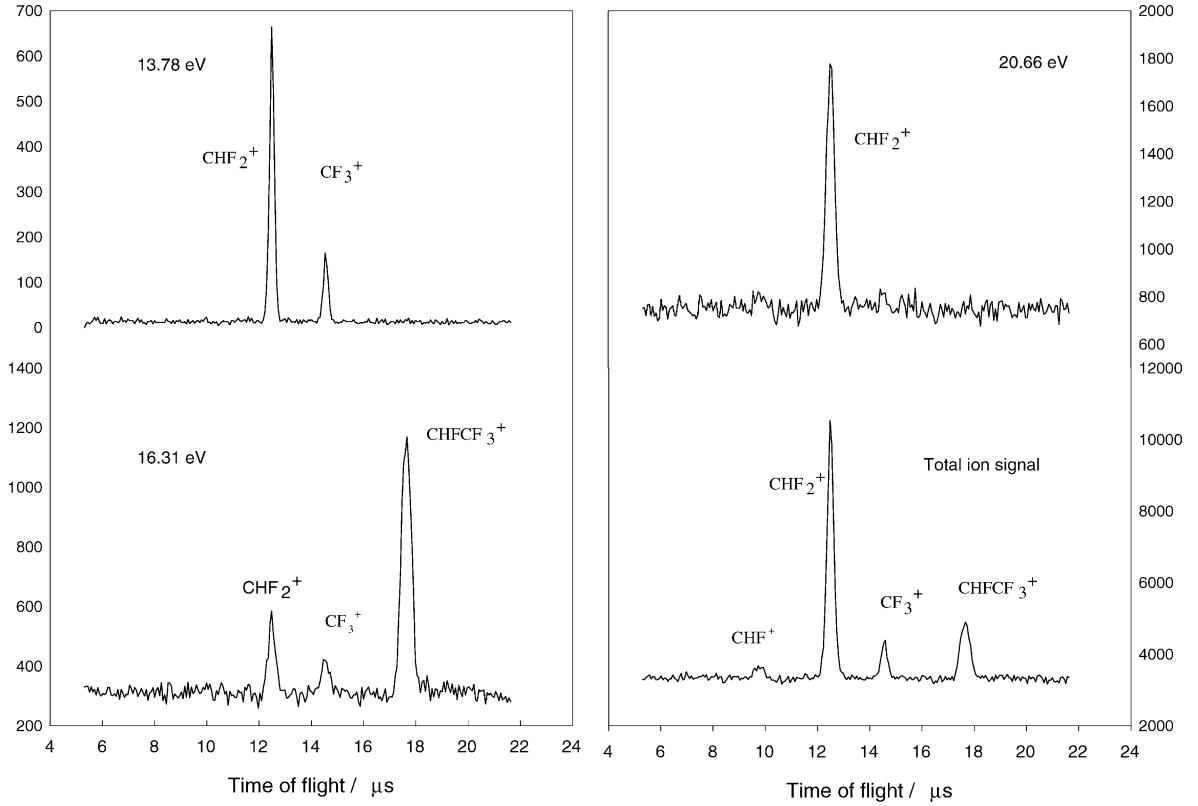

Fig. 3. TOF mass spectrum of CHF_2CF_3 recorded at energies of 13.78, 16.31, and 20.66 eV, and integrated over the complete range of 12.6–24.8 eV.

unchanged by substitution of one fluorine by one hydrogen atom.

4.2. Scanning-energy TPEPICO spectra

TPEPICO spectra were recorded as a function of photon energy from 12.6 to 24.8 eV with a constant step size of 0.19 nm. Typical TOF-MS are shown in Fig. 3, both at three different energies but also integrated over the complete energy range. As with $C_2F_6^+$, the parent ion is not observed at any energy, indicating that all valence states of $CHF_2CF_3^+$ are dissociative in the Franck–Condon region. Three main fragment ions, CHF_2^+, CF_3^+ and $CHFCF_3^+$, can clearly be identified. A fourth fragment, CHF^+, only appears weakly at higher energy, but can be identified from the summed TOF-MS. Ion yield curves for all four fragments (Fig. 2(b) and (c)) are obtained from the three-dimensional TPEPICO histogram as described earlier. From these curves, a breakdown diagram has been constructed (Fig. 4), showing the relative ion abundance as a function of photon energy from dissociative photoionisation of CHF_2CF_3.

The appearance energy (AE) at 298 K of each fragment ion has been determined from the extrapolation of the linear portion of the ion yield to zero signal. At the optical resolution of our experiment, this is equivalent to the first onset of signal. No corrections have been made for exit-channel barriers or kinetic shifts, and AEs determined in this way can only be regarded as upper limits. We have used the procedure of Traeger and McLoughlin [30] to convert an AE into an enthalpy of the unimolecular reaction at 298 K, $\Delta_r H^0_{298}$. For the reaction $AB \rightarrow A^+ + B + e^-$

$$\Delta_r H^0_{298} \leqslant AE(A^+)_{298} + \int_0^{298} c_p(A^+)\,dT + \int_0^{298} c_p(B)\,dT - \frac{5RT}{2}. \quad (1)$$

We use the stationary electron convention that, at threshold, the electron has zero translational energy. With this convention

$$\int_0^{298} c_p(e^-)\,dT = 0. \quad (2)$$

If the last three terms of Eq. (1) are ignored, a significant error may be introduced in equating the measured AE into an upper limit for $\Delta_r H^0_{298}$. The second and third terms on the right-hand side of Eq. (1), equivalent to $H^0_{298} - H^0_0$ for A^+ or B, contain contributions from translational ($2.5RT$), rotational ($1.5RT$) and vibrational ($N_A hv/[\exp(hv/k_B T) - 1]$ per vibrational mode) motion, evaluated at $T = 298$ K. The error is greater the larger the number of vibrational modes, and hence the number of atoms in A^+ and B. Vibrational frequencies of A^+ and B are taken from standard sources [31,32]. If they are not available, they are estimated by comparison with molecules having a similar number of atoms.

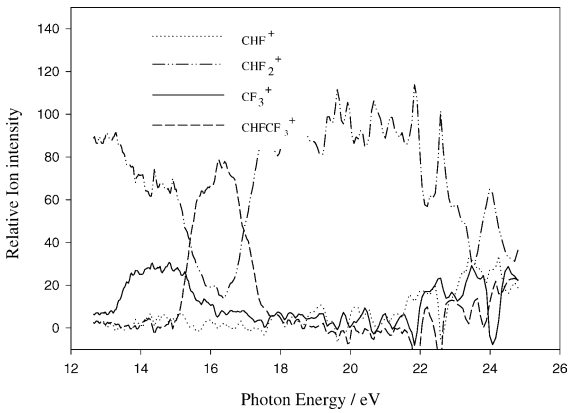

Fig. 4. Breakdown diagram for dissociative photoionisation of CHF_2CF_3.

In the region of the ground electronic state of $CHF_2CF_3^+$, the first fragment ion observed is CHF_2^+ with an AE of 12.75 ± 0.05 eV. This converts into an upper limit for the enthalpy change for the reaction $CHF_2CF_3 \rightarrow CHF_2^+ + CF_3 + e^-$ at 298 K of 12.92 ± 0.05 eV. This value is in reasonable agreement with the dissociation energy for this reaction, $\Delta_r H^0_{298} = 12.83$ eV, calculated using literature values for the 298 K enthalpies of formation for CHF_2CF_3, CHF_2^+ and CF_3 of -1100 [33], 604 [34] and -466 [35] kJ mol^{-1}, respectively. The value for CHF_2^+ is derived from the AE_{298} of CHF_2^+ from CH_2F_2 [34], with a small correction determined by the method of Traeger and McLoughlin [30]; unfortunately, this correction was not made in our original paper. With the

exception of the $\tilde{A}$ state, CHF_2^+ appears as the major fragment for dissociation of all valence states of $CHF_2CF_3^+$. The second fragment ion observed is CF_3^+ with an AE of 13.29 ± 0.06 eV, also within the Franck–Condon envelope of the ground state of $CHF_2CF_3^+$. This converts into an upper limit for the enthalpy change for the reaction $CHF_2CF_3 \rightarrow CF_3^+ + CHF_2 + e^-$ at 298 K of 13.46 ± 0.06 eV. This energy is significantly greater than the dissociation energy for this reaction at 298 K, 13.15 eV, calculated using the most recent experimental value for the enthalpy of formation at 298 K of CF_3^+, 406 kJ mol^{-1} [36], and the older literature value for CHF_2 [37]. These two fragments are the only ions produced from dissociation of the ground state of $CHF_2CF_3^+$. The greater intensity of the CHF_2^+ signal suggests that, at the instant of dissociation, the density of positive charge is located more on the $-CHF_2$ than the $-CF_3$ group. The moderate agreement of both AEs with the calculated values for $\Delta_r H^0_{298}$ suggest that these fragment ions are produced by a C–C bond cleavage with a relatively small release of translational kinetic energy.

Over the Franck–Condon region of the first excited state of $CHF_2CF_3^+$ (vertical IE = 16.37 eV), the relative yield of CHF_2^+ and CF_3^+ drops rapidly, and $CHFCF_3^+$ becomes the dominant fragment ion with a relative yield of ca. 0.8 at the Franck–Condon maximum. (Although we cannot differentiate the two isomers $CHFCF_3^+$ and $CHF_2CF_2^+$ in the TOF-MS, the ab initio calculations suggest that, for a rapid impulsive dissociation, the former is likely to be dominant, as the (HOMO-1) orbital of CHF_2CF_3 is mainly F 2pπ non-bonding on the $-CHF_2$ group.) The AE of this ion is 15.15 ± 0.07 eV. Since this energy corresponds to the onset of the $\tilde{A}$ state of $CHF_2CF_3^+$, and the ion yield of $CHFCF_3^+$ follows closely the threshold photoelectron signal over the range 15–17 eV, it is likely that $CHFCF_3^+$ is produced directly from the $\tilde{A}$-state potential energy surface without prior internal conversion to the ground state. The behaviour of this state is then characteristic of impulsive decay from an isolated electronic state, and has been observed for dissociation of the $\tilde{A}$ state of $C_2F_6^+$ [9,28,29]. This conclusion is consistent with the relatively large kinetic energy released into $CHFCF_3^+ + F$ (Section 4.3), and with the molecular orbital calculation (Section 3) that this state is produced by electron removal from a F 2pπ non-bonding orbital on the $-CHF_2$ group. Hence, as suggested by Seccombe et al. [38] for the dissociative photoionisation of $CFCl_3$, following photon excitation a localised hole is created on a F atom, favouring C–F bond fission if dissociation is impulsive and rapid.

From the AE ($CHFCF_3^+$), using the method of Traeger and McLoughlin [30] we determine $\Delta_f H^0_{298}$ ($CHFCF_3^+$) $\leqslant 299 \pm 7$ kJ mol^{-1}. However, since the fragmentation $CHF_2CF_3^+ \rightarrow CHFCF_3^+ + F$ has a considerable kinetic energy release (Section 4.3), it is likely that the true enthalpy of formation of this ion is significantly lower than this value. Recently, we have described a method to determine the dissociative ionisation energy of polyatomic molecules whose ground state of the parent ion is repulsive in the Franck–Condon region; indirectly, this is a means to determine absolute enthalpies of formation of radical cations, rather than upper limits [39]. Briefly, TPEPICO spectra at high time resolution are measured as a function of photon energy over the Franck–Condon region of the repulsive state of the parent cation. By determining the mean translational kinetic energy release, $\langle KE \rangle_T$, as a function of $h\nu$, an extrapolation can be performed to determine the photon energy at which $\langle KE \rangle_T$ would be zero. This is termed the dissociative ionisation energy of the molecule, from which the absolute enthalpy of formation of the fragment ion can be determined. We applied this technique to dissociation from the repulsive electronic ground state of CF_4^+ (to $CF_3^+ + F$), SF_6^+ (to $SF_5^+ + F$) and $CF_3SF_5^+$ (to $CF_3^+ + SF_5$) [39], and obtained enthalpies of formation of CF_3^+ and SF_5^+ in good agreement with other methods. We have attempted to apply this method to dissociative *excited* states of parent cations, in particular $C_2F_6^+$ $\tilde{A}$ (to $C_2F_5^+ + F$) and $CHF_2CF_3^+$ $\tilde{A}$ (to $CHFCF_3^+ + F$). In both cases, the results were inconclusive, and we were not able to extrapolate satisfactorily the graphs of $\langle KE \rangle_T$ vs. $h\nu$ to $\langle KE \rangle_T = 0$. There are three explanations. Either the signal-to-noise ratio of the multiple TOF spectra was not sufficient to obtain meaningful values of $\langle KE \rangle_T$. Or the main assumption of

the extrapolation method, that the dissociation mechanism at threshold is the same as in the Franck–Condon region, is invalid. Or the technique is not applicable to electronic excited states, where an alternative channel to direct impulsive dissociation is open, e.g., internal conversion to the ground state. We comment that the breakdown diagram for $CHF_2CF_3^+$ (Fig. 4) shows that, whilst $CHFCF_3^+$ is the dominant ion at the Franck–Condon maximum of $CHF_2CF_3^+$ $\tilde{A}\,^2A'$, there is still a small but significant yield of both CHF_2^+ and CF_3^+ which could result from a minor dissociation pathway via the electronic ground state of the parent ion. It was not possible, therefore, to determine an absolute value for the enthalpy of formation of $CHFCF_3^+$, for which there are no other values in the literature. We can only confirm an upper limit for $\Delta_f H^0_{298}$ ($CHFCF_3^+$) of 299 ± 7 kJ mol^{-1}.

The three fragment ions CHF_2^+, CF_3^+ and $CHFCF_3^+$ dominate the breakdown diagram up to ca. 17.5 eV. Above this energy, the $CHFCF_3^+$ signal decreases rapidly, and CHF_2^+ (or CF_2^+, since these ions are unresolvable in our TOF-MS) becomes the dominant fragment ion again. Some features in the ion yield of CHF_2^+ (or CF_2^+) can clearly be recognised, since they match closely the electronic states in the TPES. The rapid switch back to the CHF_2^+ (or CF_2^+) fragment, with the equally rapid decline of $CHFCF_3^+$ at an energy corresponding to electronic valence states of the parent ion, and the similarity of the CHF_2^+ and TPES signals may indicate impulsive behaviour in these higher valence states of $CHF_2CF_3^+$. A small yield of CHF^+ ($AE = 17.5 \pm 0.2$ eV) appears as the photon energy is increased, but the signal is very weak. It is possibly produced by secondary dissociation of CHF_2^+, with CF_4 being the neutral partner; we comment that dissociation to $CHF^+ + F + CF_3$ only becomes energetically allowed for photon energies greater than ca. 18.7 eV.

4.3. Kinetic energy releases

TPEPICO-TOF spectra at a resolution of 8 ns were recorded for the three main fragment ions at photon energies corresponding to the Franck–Condon maxima of the valence states of $CHF_2CF_3^+$. Accumulation times per spectrum ranged from 2–8 h. In our experiments, fragment ions often have enough translational energy release for the TOF peak to be substantially broadened from that expected for a thermal source of such ions [40]. Analysis of the shape of such TOF peaks allows a determination of the kinetic energy release distribution (KERD), and hence the total mean translational kinetic energy release, $\langle KE \rangle_T$, associated with a particular dissociation process. The thermal energy of the parent molecule at 298 K is convoluted into each component of the KERD, and the analysis is only applicable to a two-body process, corresponding to the fission of one bond. Full details are given elsewhere [23,24]. The value of $\langle KE \rangle_T$ can be divided by the available energy, E_{avail}, defined as the photon energy minus the thermochemical dissociation energy, to determine the fraction of the available energy being channelled into translational energy of the two fragments, f_T.

It is informative to determine whether a polyatomic ion dissociates in a statistical or impulsive manner. Statistical dissociation is characterised by a parent ion excited to an electronic state which is so long lived that energy randomisation occurs prior to dissociation. Internal conversion can occur to the electronic ground state, and dissociation proceeds from that potential energy surface. This results in a relatively low fractional kinetic energy release, the amount decreasing as the size of the parent ion increases. Klots [41] has then shown that $\langle KE \rangle_T$ and E_{avail} are related by a simple analytical expression:

$$E_{avail} = \frac{(r-1)}{2}\langle KE \rangle_T + \langle KE \rangle_T + \sum_i \{h\nu_i/(\exp(h\nu_i/\langle KE \rangle_T) - 1)\}, \quad (3)$$

where r is the number of rotational degree of freedoms, and ν_i is the vibrational frequency of the ith vibrational mode of the daughter ion. In this model, it is assumed that energy and angular momentum are conserved, and the available energy is large enough that any exit-channel barrier to products can be neglected. Such dissociations also assume that the electronic ground state of the parent ion is bound, at least in some regions of its

multi-dimensional surface, and knowledge of the vibrational frequencies of the daughter ion is required. If these values are not known, a lower limit to f_T, $1/(x+1)$, can be estimated [42], where x is the number of vibrational degrees of freedom in the transition state of the unimolecular dissociation. For $CHF_2CF_3^+$ with eight atoms, $x = 3N - 7$ or 17, leading to a predicted $f_T \geqslant 0.06$.

Impulsive dissociation is characterised by a short-lived electronic state of the parent ion which fragments on a time scale comparable to or faster than that of internal molecular motion, intramolecular vibrational redistribution, or electronic relaxation. Dissociation proceeds along a pseudo-diatomic exit channel of the potential energy surface of the particular electronic state. For the pure-impulsive model, it is assumed that the two atoms surrounding the breaking bond recoil with such force that dissociation results in intramolecular collisions between the excited atom and the remainder of their recoiling fragments. As a consequence, there is a transfer of energy to vibrational, in addition to the possible transfer of energy to rotational, degrees of freedom of the fragments. For this model, Holdy et al. [43] have shown that E_{avail} and $\langle KE \rangle_T$ are related by simple kinematics

$$f_T = \frac{\langle KE \rangle_T}{E_{avail}} = \frac{\mu_b}{\mu_f}, \quad (4)$$

where μ_b is the reduced mass of the two atoms whose bond is broken and μ_f is the reduced mass of the two fragments formed from the dissociation. For the modified-impulsive model [44], repulsion of the two atoms is not sufficient to cause energy transfer to the vibrational modes of the fragments. They recoil as rigid bodies, no energy is partitioned into vibrational modes of the fragments, and f_T is somewhat higher.

The experimentally determined values of $\langle KE \rangle_T$ and f_T are shown in Table 2, together with calculated values of f_T for statistical and pure-impulsive dissociation models. For fragmentation of $CHF_2CF_3^+$ $\tilde{A}\ ^2A'$ to $CHFCF_3^+ + F$ at 16.37 eV, the TPEPICO-TOF spectrum is shown in Fig. 5. The experimental value of f_T, 0.67, agrees reasonably well with the value based on the pure-impulsive model, 0.46. This observation is consistent with the arguments presented in Section 4.2, and shows that the $\tilde{A}\ ^2A'$ state of the parent ion shows isolated-state behaviour, similar to that of the first excited state of $C_2F_6^+$ [9,28,29]. There are two possible explanations why the experimental value of f_T is greater than that predicted by the pure-impulsive model. Either dissociation follows the modified-impulsive model, or E_{avail} is greater than that calculated from $AE_{298}(CHFCF_3^+)$ since $\Delta_f H^0_{298}(CHFCF_3^+)$ is significantly less than 299 kJ mol^{-1}. Since f_T is so high, however, this is good

Table 2
Mean translation kinetic energy releases, $\langle KE \rangle_T$, for the two-body fragmentation of $CHF_2CF_3^+$ at photon energy $h\nu$

Ion	$h\nu$ (eV)	E_{avail} (eV)[a]	$\langle KE \rangle_T$ (eV)	Fraction ratio[c]		
				Experimental	Statistical	Impulsive
CHF_2^+	13.78	0.95	0.06 ± 0.01	0.06	0.06	0.20
	16.37	3.54	0.22 ± 0.01	0.06	0.06	0.20
	17.46	4.63	0.15 ± 0.01	0.03	0.06	0.20
	19.68	6.85	0.34 ± 0.01	0.05	0.06	0.20
	21.19	8.36	0.51 ± 0.02	0.06	0.06	0.20
	23.39	10.56	0.59 ± 0.02	0.06	0.06	0.20
CF_3^+	13.78	0.59	0.06 ± 0.01	0.10	0.06	0.20
	16.37	3.18	0.22 ± 0.01	0.07	0.06	0.20
	23.39	10.20	0.58 ± 0.02	0.06	0.06	0.20
$CHFCF_3^+$	16.37	1.05[b]	0.70 ± 0.03	0.67	0.06	0.46

[a] $E_{avail} = h\nu$ – calculated thermochemical dissociation energy (Section 4.2).
[b] $E_{avail} = h\nu - AE_{298}(CHFCF_3^+/CHF_2CF_3)$ corrected for thermal effects by the procedure of Traeger and McLoughlin [30].
[c] Given by $\langle KE \rangle_T / E_{avail}$.

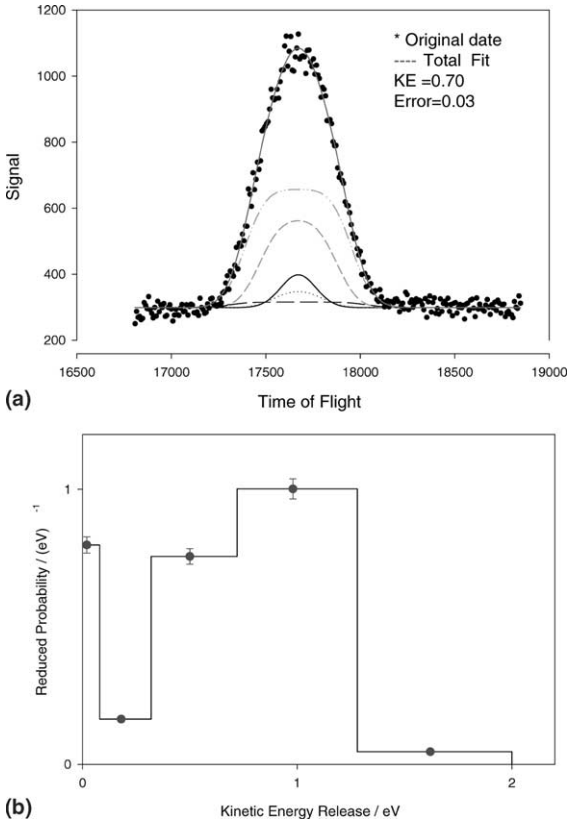

Fig. 5. Coincidence TOF spectrum (dots) of $CHFCF_3^+$ from CHF_2CF_3 photoionised at 16.37 eV. The solid line gives the best fit to the data, comprised of five contribution ($n = 1, 2, 3, 4, 5$) in the basis set for $\varepsilon_t(n)$ [24]. The reduced probability of each contribution is shown in (b). The fit yields a total mean translational kinetic energy, $\langle KE \rangle_T$, into $CHFCF_3^+ + F$ of 0.70 ± 0.03 eV which constitutes 67% of the available energy.

evidence that the structure of $CHFCF_3^+$ is similar to that part of the moiety in $CHF_2CF_3^+$.

For formation of CHF_2^+ and CF_3^+ over a wide range of energies, the much lower values of f_T for both ions might suggest that a statistical decay mechanism is operating. For the ground state of $CHF_2CF_3^+$, this seems unlikely, since the absence of parent ion signal in the TPEPICO TOF-MS spectra implies that this state is not bound in the Franck–Condon region. Mitchell and Simons [45], however, have shown that impulsive dissociation can cause a much lower value of $\langle KE \rangle_T$ and f_T than the interfragment impulsive models suggest, if one of the bond lengths or bond angles in the fragment ion is considerably different from its value in the parent ion. Such an *intrafragment* mechanism results in the daughter ion and/or the neutral fragment having significant amounts of vibrational excitation. The most likely candidate for both CHF_2^+ and CF_3^+ is the umbrella mode, ν_2, due to these groups being pyramidal when located in the parent ion but planar in the isolated ion. There is then a large change in the degree of planarity of the receding fragments in the impulsive fragmentation. From the kinetic energy data, therefore, it is not possible to determine whether higher electronic states of $CHF_2CF_3^+$ above 17.5 eV dissociate to $CHF_2^+ + CF_3$ in a statistical or an impulsive manner, since it is possible to account for the low values of f_T by both mechanisms.

5. Conclusions

We have recorded the threshold photoelectron and TPEPICO spectra of CHF_2CF_3 over the energy range 12–25 eV. Ion yield curves and the breakdown diagram have been determined. The mean translational kinetic energy release into dissociation channels involving a single bond cleavage from $(CHF_2CF_3^+)^*$ have been measured. Ab initio G2 molecular orbital calculations have determined the minimum-energy geometries of CHF_2CF_3 and its cation, and deduced the character of the highest-lying valence orbitals of the neutral molecule. Combining experimental and theoretical data, the decay mechanisms of the ground and several excited valence states of $CHF_2CF_3^+$ have been determined. Decay from the $\tilde{A}\ ^2A'$ state of the parent ion occurs impulsively by C–F bond fission to $CHFCF_3^+ + F$. The geometry of the daughter ion is not significantly different from that of this ion in $CHF_2CF_3^+$. The ground and higher-lying states of $CHF_2CF_3^+$ dissociate by C–C fission to both CHF_2^+ and CF_3^+, with the former ion dominant. From the kinetic energy data, it is not possible to deduce unambiguously the mechanism of these reactions, although it seems likely that dissociation from the ground state of $CHF_2CF_3^+$ is not statistical, due to the absence of parent ion signal in the TPEPICO

spectrum at this energy. An improved value is determined for the enthalpy of formation at 298 K of the $CHFCF_3^+$ cation.

Acknowledgements

We thank EPSRC for a Postdoctoral Fellowship (W.Z.), studentships (D.P.S. and M.K.T.) and research grants, including beamtime at the Daresbury SRS. We thank Mr. R.Y.L. Chim for helpful discussions and a critical reading of the manuscript.

References

[1] Scientific assessment of ozone depletion (World Meteorological Organisation/United Nations Environmental Programme) 1994, Report No.37.
[2] T.J. Wallington, O.J. Nielsen, Progress in Atmospheric Chemistry, World Scientific, Singapore, 1995 (chapter 15).
[3] J. Berkowitz, G.B. Ellison, D.J. Gutman, J. Phys. Chem. 98 (1994) 2744.
[4] S. Papasavva, S. Tai, A. Esslinger, K.H. Illinger, J.E. Kenny, J. Phys. Chem. 99 (1995) 3438.
[5] Y.H. Chen, S.J. Paddison, E. Tschuikow-Roux, J. Phys. Chem. 98 (1994) 1100.
[6] J.R. Durig, J. Liu, T.S. Little, V.F. Kalasinsky, J. Phys. Chem. 96 (1992) 8224.
[7] T. Heinis, R. Bar, K. Borlin, M. Jungen, Chem. Phys. 94 (1985) 235.
[8] D. McNaughton, C. Evans, E.G. Robertson, J. Chem. Soc. Faraday Trans. 91 (1995) 1723.
[9] G.K. Jarvis, K.J. Boyle, C.A. Mayhew, R.P. Tuckett, J. Phys. Chem. A 102 (1998) 3219.
[10] G.K. Jarvis, K.J. Boyle, C.A. Mayhew, R.P. Tuckett, J. Phys. Chem. A 102 (1998) 3230.
[11] A. Danti, J.L. Wood, J. Chem. Phys. 30 (1959) 582.
[12] T. Yamada, T.H. Lay, J.W. Bozzelli, J. Phys. Chem. A 102 (1998) 7286.
[13] R.D. Parra, X.C. Zeng, J. Phys. Chem. A 102 (1998) 654.
[14] M.R. Zachariah, P.R. Westmoreland, D.R. Burgess, W. Tsang, J. Phys. Chem. 100 (1996) 8737.
[15] A.S. Hasson, C.M. Moore, I.W.M. Smith, J. Chem. Soc., Trans. 93 (1997) 2693.
[16] A.B. Tipton, C.O. Britt, J.E. Boggs, J. Chem. Phys. 46 (1967) 1606.
[17] F.B. Brown, A.D.H. Clague, N.D. Heitkamp, D.F. Koster, A. Danti, J. Mol. Spectrosc. 24 (1967) 163.
[18] S. Eltayeb, G.A. Guirgis, A.R. Fanning, J.R. Durig, J. Raman Spectrosc. 27 (1996) 111.
[19] L.A. Curtiss, K. Raghavachari, G.W. Trucks, J.A. Pople, J. Chem. Phys. 94 (1991) 7221.
[20] P.A. Hatherly, M. Stankiewicz, K. Codling, J.C. Creasey, H.M. Jones, R.P. Tuckett, Meas. Sci. Technol. 3 (1992) 891.
[21] P.A. Hatherly, D.M. Smith, R.P. Tuckett, Z. Phys. Chem. (Munich) 195 (1996) 97.
[22] W.C. Wiley, I.H. Maclaren, Rev. Sci. Instrum. 26 (1955) 1150.
[23] I. Powis, P.I. Mansell, C.J. Danby, Int. J. Mass Spectrom. Ion Phys. 32 (1979) 15.
[24] G.K. Jarvis, D.P. Seccombe, R.P. Tuckett, Chem. Phys. Lett. 315 (1999) 287.
[25] B. Beagley, M.O. Jones, P. Yavari, J. Mol. Struct. 71 (1981) 203.
[26] e.g. M. Horn, M. Oswald, R. Oswald, P. Botschwina, Ber. Buns. Phys. Chem. 99 (1995) 323.
[27] P. Sauvageau, J. Doucet, R. Gilbert, C. Sandorfy, J. Chem. Phys. 61 (1974) 391.
[28] M.G. Inghram, G.R. Hanson, R. Stockbauer, Int. J. Mass Spectrom. Ion Phys. 33 (1980) 253.
[29] I.G. Simm, C.J. Danby, J.H.D. Eland, Int. J. Mass Spectrom. Ion Phys. 14 (1974) 285.
[30] J.C. Traeger, R.G. McLoughlin, J. Am. Chem. Soc. 103 (1981) 3647.
[31] M.W. Chase, J. Phys. Chem. Ref. Data (1998), monograph no. 9.
[32] http://webbook.nist.gov (NIST website).
[33] D.R. Lide (Ed.), CRC Handbook of Chemistry and Physics, 78th ed., CRC press, Boca Raton, FL, 1998.
[34] D.P. Seccombe, R.P. Tuckett, B.O. Fisher, J. Chem. Phys. 114 (2001) 4074.
[35] B. Ruscic, J.V. Michael, P.C. Redfern, L.A. Curtiss, K. Raghavachari, J. Phys. Chem. A 102 (1998) 10889.
[36] G.A. Garcia, P.M. Guyon, I. Powis, J. Phys. Chem. A 105 (2001) 8296.
[37] S.G. Lias, J.E. Bartmess, J.F. Liebman, J.L. Holomes, R.D. Levin, W.G. Mallard, J. Phys. Chem. Ref. Data 17 (Suppl. 1) (1988).
[38] D.P. Seccombe, R.Y.L. Chim, G.K. Jarvis, R.P. Tuckett, Phys. Chem. Chem. Phys. 2 (2000) 769.
[39] R.Y.L. Chim, R.A. Kennedy, R.P. Tuckett, W. Zhou, G.K. Jarvis, D.J. Collins, P.A. Hatherly, J. Phys. Chem. A 105 (2001) 8403.
[40] J.L. Franklin, P.M. Hierl, D.A. Whan, J. Chem. Phys. 47 (1967) 3148.
[41] C.E. Klots, J. Chem. Phys. 58 (1973) 5364.
[42] J.L. Franklin, Science 193 (1976) 725.
[43] K.E. Holdy, L.C. Klots, K.R. Wilson, J. Chem. Phys. 52 (1970) 4588.
[44] G.E. Busch, K.R. Wilson, J. Chem. Phys. 56 (1972) 3626.
[45] R.C. Mitchell, J.P. Simons, Discuss. Faraday Soc. 44 (1967) 208.